Advances in Colloid and Interface Science 275 (2020) 102077

Contents lists available at ScienceDirect

Advances in Colloid and Interface Science

journal homepage: www.elsevier.com/locate/cis

Historical Perspective

Polymer-mediated colloidal stability: on the transition between adsorption and depletion

Álvaro González García [a,b,1], Marjolijn M.B. Nagelkerke [a,b,1], Remco Tuinier [b,a,*,1], Mark Vis [b,1]

[a] Van 't Hoff Laboratory for Physical and Colloid Chemistry, Department of Chemistry & Debye Institute, Utrecht University, Padualaan 8, 3584 CH, Utrecht, the Netherlands
[b] Laboratory of Physical Chemistry, Department of Chemical Engineering and Chemistry & Institute for Complex Molecular Systems (ICMS), Eindhoven University of Technology, P.O. Box 513, 5600 MB Eindhoven, the Netherlands

ARTICLE INFO

Article history:
18 November 2019
Available online 21 November 2019

Keywords:
Colloid–polymer mixtures
Depletion
Adsorption
Colloidal interaction
Bridging
Phase behavior

ABSTRACT

Addition of polymers to a colloidal dispersion modulates the interactions between the colloids. We briefly review the effects of positive and negative adsorption (also termed depletion). The effective colloid–polymer interactions sensitively affect the colloidal phase behavior. We present a theoretical framework to predict the phase behavior of colloid–polymer mixtures for varying affinities between colloid and polymer, leading to either positive or negative adsorption of polymer segments. For certain conditions, polymers are neither depleted nor adsorbed: the polymer concentration is essentially constant up to the colloidal surface, a condition which we term neutral adsorption. Near this condition, the calculated phase diagrams reveal a stable–unstable–restabilisation transition with increasing polymer concentration. Similar effects have been reported experimentally, for instance as a function of temperature [Feng et al., *Nat. Mat.*, 2015, **14**, 61–65], which may modulate the effective polymer–colloid affinity. Understanding how to achieve neutral adsorption opens up the possibility of preparing highly dense, yet stable, colloid–polymer mixtures.

Contents

1. Introduction . . . 1
2. Methods . . . 3
3. Polymers near surfaces . . . 4
4. Pair interactions and second virial coefficient . . . 5
5. Phase diagrams . . . 6
6. Conclusions . . . 8
Acknowledgement . . . 8
Appendix A. FMSA for HCY potentials . . . 8
Appendix B. Pair potentials at various conditions . . . 8
Appendix C. Re-entrant F–S phase behavior at fixed colloid volume fraction . . . 8
References . . . 8

1. Introduction

About four millennia ago the Egyptians desired to write and as a result invented classic ink: carbon black particles dispersed in water, together with biopolymers [1]. The presence of the latter, either in the form of milk caseins, egg white albumin, or gum arabic from the *Acacia* tree resulted in colloidal stability of the ink dispersion. Since carbon black particles do not disperse in water without a layer of stabilizing polymers, the Egyptians obviously were already capable of achieving steric stabilization.

One century ago scientists gradually started to gain insights into the properties of colloidal particles in solvents. The stability of aqueous colloidal dispersions gained significant attention. The colloidal stability of

* Corresponding author at: Laboratory of Physical Chemistry, Department of Chemical Engineering and Chemistry, Institute for Complex Molecular Systems (ICMS), Eindhoven University of Technology, P.O. Box 513, 5600, MB, Eindhoven, the Netherlands.
E-mail address: r.tuinier@tue.nl (R. Tuinier).
[1] All authors contributed equally.

https://doi.org/10.1016/j.cis.2019.102077

such charged particle dispersions strongly depended on salt concentration. The independent but simultaneous efforts in the USSR by Boris Derjaguin and Lev Landau in Moscow, and by Evert Verwey and Theo Overbeek in Eindhoven, the Netherlands, led to a framework, often termed DLVO theory [2,3], which provides a semi-quantitative description of the interactions and stability of charged colloids in polar solvents. It became clear that van der Waals interactions between the colloidal particles in a solvent lead to attraction between the particles, while double layer interactions typically result in repulsive interactions. The latter depend on salt concentration, which clarified the finding that aqueous colloids may aggregate at high salt content.

Later work commenced on the influence of additives such as polymer chains or a second kind of colloid.[2] In the 1950s Sho Asakura and Fumio Oosawa [4,5] in Nagoya, Japan, showed that adding nonadsorbing macromolecules to a colloidal dispersion induced effective attractions between the colloidal particles. In the same period E.W. Fischer [6] in Mainz, Germany, demonstrated that the presence of polymers at the surface of colloids can lead to steric stabilization and are capable of compensating van der Waals attractions. For an early review on the effects of polymer adsorption, see for instance Ref. 7.

Hans Lyklema, who finished his PhD study under the guidance of professor Overbeek in 1957, initiated a line of research at Wageningen University which was largely dedicated to (positive and negative) adsorption of ions, proteins, polymers, and surfactants onto colloidal particles. Adsorption is the excess of a compound at an interface with respect to its bulk concentration. The PhD thesis of his student Gerard Fleer [8] may be regarded as pioneering work on experimental polymer adsorption studies [9–11]. One may say that this work in the end helped to initiate the development of the Scheutjens–Fleer self-consistent field theory to study polymers near interfaces [12,13], as well as many other topics and extensions [14] including the effects of charges [15,16].

Mixtures of colloidal particles and polymers are not only of fundamental interest but are widespread in biological [17–19] (e.g., blood) and industrial [20,21] (e.g., paint) systems. Fundamental understanding of the colligative properties of colloid–polymer mixtures (CPMs) in terms of the molecular parameters involved provides a design pathway towards the desired final application. Particularly, the solvent quality [22,23] as well as the specific polymer–colloid interaction [24] mediate the stability of the CPM. Polymers which do not adsorb onto the colloidal particles cause an indirect, *entropy-driven* attraction between the colloids, known as the depletion attraction [24]. On the other hand, polymer adhesion driven by *enthalpic* attractions between the polymer and the colloid leads to flocculation at low polymer concentrations and steric stabilization at higher concentrations [25]. It is clear that both polymer depletion as well as polymer adhesion phenomena strongly mediate colloidal stability.

Fig. 1 sketches expected situations emerging upon adding polymer chains to a dispersion of colloidal particles in a common solvent. In the case of negative adsorption or, as Napper probably first coined [26,27], depletion there are excluded volume layers surrounding the colloidal spheres in which the concentration of polymer segments of polymer chains is smaller than in the bulk (Fig. 1a–c). Negative adsorption implies that the polymer segment concentration in the vicinity of the colloidal particles is lower than in the bulk. The extent of this region is denoted as the depletion thickness and is in a dilute polymer solution close the radius of gyration of the polymer chains [28]. Theory [29], experiments [22], and computer simulation [30] studies have revealed that the depletion thickness decreases at sufficiently high polymer concentrations.

[2] In classical colloid chemistry the term 'colloid' refers to a colloidal dispersion (colloidal particles plus medium). Here, we use it also to refer to the colloidal particles.

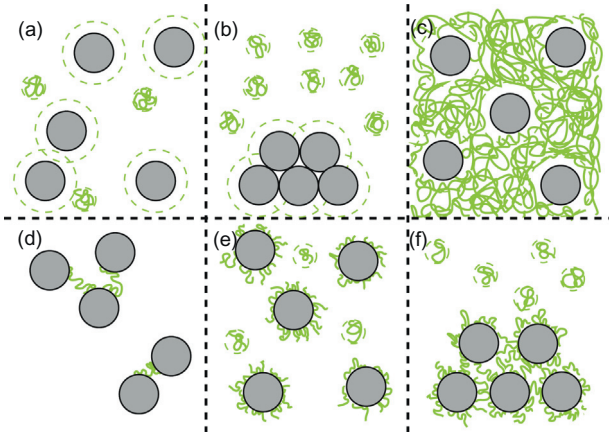

Fig. 1. Schematic scenarios occurring after mixing polymers (green chains) with colloidal spheres (grey particles) in case of (a–c) negative adsorption (depletion) of polymers or (d–f) positive adsorption (accumulation) of polymers.

Whenever the depletion zones of colloids overlap the osmotic pressure of the nonadsorbing polymers gets unbalanced, pushing the particles together. Therefore the presence of the depletion zones leads to an effective attraction between the colloidal spheres, which can be explained by the fact that the total volume of the depletion zones can be reduced if they overlap [31]. In the case of low polymer concentration (a) the attraction is too weak to cause any instability. Upon increasing the polymer concentration (b) the attraction can get strong to such a degree that the mixture becomes unstable and phase separation takes place, leading to (for instance) two coexisting phases: one enriched in polymer chains and another phase enriched in colloidal particles. At very high concentrations (far above the polymer overlap concentration) the depletion thickness may become so thin that the system restabilizes (c) [26,27,32].

In case of accumulation of polymer chains the situation is quite different (Fig. 1d–f). If there is a relatively small amount of positively adsorbing polymer chains the polymer coils tend to adhere onto multiple surfaces, thereby inducing bridging flocculation (d) [33]. When the amount of polymers added is sufficient to completely cover all particle surfaces the dispersion may be stable (e): there can be sufficient steric repulsion between the adsorbed polymer layers to prevent any flocculation [34]. Still, upon overdosing the amount of polymers depletion forces become significant, again leading to demixing (f) [35].

Instability of CPMs is often undesirable since long-term stability is a requirement for products such as food and coatings. It should be mentioned however that phase separation can also be useful to fractionate compounds or extract certain components [28]. Hence, a better understanding of the stability of CPMs, which is sensitive to both polymer depletion or adhesion phenomena, will enable to improve products and controlling related processes.

Most of the theoretical investigations on the phase behavior of CPMs have been conducted on the depletion case, particularly under the assumption that the polymer concentration *at* the colloidal surface is strictly zero [36–38]. We term this situation *classical depletion*. Such a full depletion situation is formally restricted to a particular situation. Only if the effective interaction between the polymer segments and the surface is sufficiently repulsive there is a vanishing polymer segment concentration at the colloid [39]. Whenever the entropic or enthalpic penalty for the presence of polymers near the colloidal surface is insufficient, there is a finite polymer concentration at the colloidal surface. Attention has been paid to understand the effect of this *weak depletion* as compared to the classical depletion case [22,23,40], also at high polymer concentrations [41].

Limited attention has been paid to the colloidal interactions induced by *weakly adhesive* polymers [38,42]. For polymers which weakly (reversibly) adhere onto the colloidal particle ('weak physisorption'), segment–surface attractions are smaller than the thermal energy. In this case, the phase behavior of the CPM can be interpreted using thermodynamic descriptions such as the sticky hard sphere model [43,44].

If the polymer affinity for the colloidal particle is sufficiently high, kinetic effects become relevant and/or polymers may irreversibly adsorb at the colloidal particles [25,45]. Both for depletion and bridging attraction, short-ranged and strong interactions may induce non-equilibrium phenomena. These include flocculation, aggregation, gelation [46], formation of percolated networks [42] and formation of colloidal glasses [47]. These states are out of the scope of the present work, where we present a theoretical framework for the *equilibrium* phase behavior from classical depletion to weak adsorption (situations schematized in Fig. 2).

This paper is dedicated to the line of research on polymer adsorption initiated by Hans Lyklema, and is inspired by the classic studies of two of his PhD students Jan Scheutjens and Gerard Fleer on polymer-mediated interactions between two parallel plates [48,49]. Theoretically, we first revisit the well-established negative adsorption (depletion) and (positive) adsorption polymer concentration profiles near a hard surface for a dilute polymer solution. Then, we systematically vary the polymer–colloid affinity, which reveals a smooth transition from negative to positive adsorption. In between we find a scenario of *neutral* adsorption where the polymer solution appears effectively unaffected by the colloidal particle. Neutral adsorption reveals the possibility of preparing CPMs which are stable over a wide range of polymer concentrations. From the plate–plate interactions, we resolve the polymer-mediated pair potentials between colloidal hard spheres. Following the ideas of the extended law of corresponding states [50] allows us to construct the phase diagrams of CPMs ranging from classical depletion (negative adsorption) to weak adhesion via the neutral adsorption condition.

In the next Section the framework of the computational approach followed is outlined. In the subsequent Section 3 the focus is on density profiles of polymer chains for several conditions, ranging from negative adsorption towards positive adsorption. In Section 4 results for the pair interactions between two particles mediated by the polymer chains are discussed, while the phase behavior of colloid–polymer mixtures is treated in Section 5. Finally, the conclusions are summarized in Section 6.

2. Methods

In this paper we use the Scheutjens–Fleer self-consistent mean-field theory (SCFT) for polymers at interfaces [12,51,52], and use the sfbox software for obtaining homopolymer segment distributions and plate–plate interactions. As the SCFT computations are based on Flory–Huggins (FH) mean-field theory, segment–segment interactions are captured via FH χ-parameters. We use a planar lattice with coordination number $k = 6$ (a simple cubic lattice), and account for concentration gradients in the direction orthogonal to the flat surface. The lower and upper boundary conditions of the lattice can be defined either as a solid or as a mirror. In this work, we consider two cases: i) a solid surface impenetrable to all components in the system before the first lattice layer and a mirror located after the last lattice layer, or ii) an impenetrable solid surface both before the first and after the last lattice layers. In either case, the number of layers is N_{lat}. For situation (i) $h = 2bN_{lat}$, where h is the distance between the two hard plates and b the lattice layer spacing. In case (ii), $h = bN_{lat}$. The [guest (G)] homopolymer chains added to the colloidal suspension are considered to be in a θ-solvent (W); the polymer segment–solvent interaction is $\chi_{GW} = 0.5$. The effective affinity of the polymer segments for the surface groups at a flat wall, which represents the surface of the colloidal (C) particle, is determined by the difference between polymer–colloid (χ_{CG}) and solvent–colloid (χ_{CW}) interactions. The effective interaction between the flat plate and a polymer segment (G) is therefore set via $\Delta\chi = \chi_{CG} - \chi_{CW}$. For a fixed value of χ_{GW}, results are invariant at a fixed $\Delta\chi$ [22]. For simplicity, we set $\chi_{CW} = 0$, so $\Delta\chi \equiv \chi_{CG}$. All interactions are expressed in units of k_BT, with k_B the Boltzmann constant and T the absolute temperature.

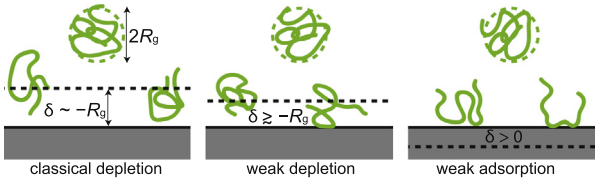

Fig. 2. Schematic representation of polymer configurations near a hard surface. Dashed lines represent the adsorption thickness δ, which is negative for depletion and positive for adsorption.

The SCFT approach provides the polymer segment concentration profile that optimizes the free energy of the lattice at the imposed values for ϕ_G^{bulk} and N_{lat}, following a semi-grand canonical approach at a fixed polymer bulk concentration. For each species the chemical potential in the bulk and in the system are equal. In the planar lattice, the resulting grand-canonical potential Ω comprises the free energy and the chemical potential of components in the lattice. Under θ-solvent conditions, the (guest) homopolymer size may be characterized via its radius of gyration [53]:

$$R_g = b\sqrt{\frac{N}{6}}, \tag{1}$$

with b the size of a lattice site and N the number of polymer segments. We set $N = 1000$ for all calculations in this work unless otherwise indicated. As no long-ranged interactions (e.g., electrostatics) play a role and we normalize all distances either by the polymer size R_g or the colloidal diameter σ, there is no need to specify b. We express the homopolymer concentration ϕ_G relative to the overlap concentration ϕ_G^*, defined as:

$$\phi_G^* = \frac{Nb^3}{v_G} \approx 3.5N^{-1/2}, \tag{2}$$

with

$$v_G = \frac{4\pi}{3}R_g^3 \tag{3}$$

the volume occupied by a polymer coil in the bulk at low concentrations. The interaction energy W_{plate} per unit area between two plates separated a distance h follows as [48]:

$$W_{plate}(h) = \Omega(h) - \Omega(\infty). \tag{4}$$

We employ the Derjaguin approximation to obtain the interaction W between two spheres from the interaction between two plates [28]:

$$W(r) = W_{HS}(r) + \frac{\pi\sigma}{2}\int_r^\infty W_{plate}(r' - \sigma)\mathrm{d}r', \tag{5}$$

where r is the distance between the centres of the colloidal spheres with diameter σ and W_{HS} is the hard-sphere (HS) potential which accounts for impenetrability between the colloidal particles (see Appendix A). An important quantity is the polymer–to–colloid size ratio q, defined as

$$q \equiv \frac{2R_g}{\sigma}. \tag{6}$$

Here we use $q = 0.15$. The interaction potentials calculated via SCFT (upon applying the Dejarguin approximation) are fitted to a hard-core Yukawa (HCY, see Appendix A) potential upon imposing the additional

constraint that for the SCFT approach and the HCY fit both the second virial coefficient B_2 and area under the potential are equal. The second virial coefficient resulting from sphero-symmetric interactions containing a hard-core contribution reads as:

$$\frac{B_2}{v_c} = 4 + 12\int_{\tilde{r}=1}^{\tilde{r}=\infty} \tilde{r}^2(1-\exp[-\beta W(\tilde{r})])\mathrm{d}\tilde{r}, \tag{7}$$

where $\tilde{r} = r/\sigma$ and $\beta = 1/(k_BT)$. From Eq. (7) it follows that for HSs $B_2 = 4v_c$ [54]. An advantage of fitting the numerical polymer-mediated colloid–colloid interactions via HCY potentials is that closed-form expressions for the thermodynamics of the colloid–polymer mixture of interest become available, see Appendix A. Given a certain choice for q, fitted ranges q_Y and strengths ε of the polymer-mediated effective colloid–colloid interaction are obtained as a function of ϕ_G^{bulk}.

3. Polymers near surfaces

Next, the focus is on density profiles near solid surfaces and the influence of the effective polymer–colloid affinity. We first consider polymers on a planar lattice where a single hard surface, which mimics the surface of the colloidal particle, is present. The resulting polymer concentration profiles already provide a first assessment of the polymer-mediated interactions between colloidal particles. For various values of the colloid–polymer affinity $\Delta\chi$, illustrative polymer segment concentration profiles near a single hard plate are plotted in Fig. 3 for a dilute polymer bulk concentration ($\phi_G^{bulk}/\phi_G^* = 10^{-4}$). Expected homopolymer segment concentration profiles [52] near a hard wall for the depletion and adhesion cases are recovered for $\Delta\chi = +1.0$ and $\Delta\chi = -0.74$, respectively. Formally, the adsorbed amount Γ (number of monomers per unit area) at a single surface is defined as [52]:

$$\Gamma = \frac{1}{b^3}\int_0^\infty \mathrm{d}z\left[\phi_G(z) - \phi_G^{bulk}\right], \tag{8}$$

where z represents the distance to the surface. The colored areas hence represent the negative (purple for $\Delta\chi = -0.4$ or purple plus grey for $\Delta\chi = +1.0$) and positive (orange, $\Delta\chi = -0.74$) adsorbed amounts of polymer segments. For $\Delta\chi = +1.0$ there is negative adsorption; the segment concentration close to the surface is smaller than in the bulk. This case is close to classical depletion of polymer chains at the colloidal surface, for which $\phi_G(z=0) \approx 0$. For

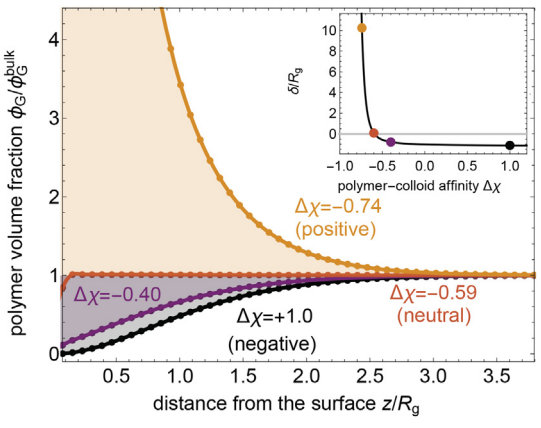

Fig. 3. Polymer concentration profiles relative to bulk (ϕ_G/ϕ_G^{bulk}) as a function of the distance from a flat surface (z/R_g). Polymer–colloid affinities $\Delta\chi$ as indicated. In the inset, the adsorption thickness δ as a function of $\Delta\chi$ is presented. The situation $\delta \approx 0$ corresponds to the neutral adsorption condition. Polymer bulk concentration relative to overlap is $\phi_G^{bulk}/\phi_G^* = 10^{-4}$. The polymer consists of $N = 1000$ segments with segment–solvent interaction $\chi_{GW} = 0.5$.

$z > 0$, the segment concentration gradually increases until it reaches the plateau bulk value, reached near $z \approx 3R_g$. A precise evaluation for $\phi_G(z=0) = 0$ corresponds to $\Delta\chi = 6\ln(7/6) \approx +0.92$ [55]. As can be observed, for $\Delta\chi = -0.4$ the segment concentration at the surface is finite and the segment density profile is narrower than for $\Delta\chi = +1.0$.

For adhesive polymers ($\Delta\chi = -0.74$), the concentration near the colloidal hard surface is much greater than in bulk, and reaches its bulk value also around $z \approx 3R_g$. The equilibrium properties of adsorbed polymers[3] are well-established [56], and the features of weakly-adsorbing polymers are well-recovered in SCFT [52].

Remarkably, for $\Delta\chi \approx -0.59$ the polymer segment concentration profile is practically equal to ϕ_G^{bulk} up to the lattice site adjacent to the hard surface. This specific colloid–polymer affinity defines the neutral adsorption condition, characterized by polymers that are neither depleted from nor adhered at the hard surface (see Fig. 2). In the inset of Fig. 3 we show the adsorption thickness δ of the polymer, defined as $\delta = b^3\Gamma/\phi_G^{bulk}$ or, in a discrete lattice approach:

$$\frac{\delta}{b} = \sum_z \frac{\phi_G(z)}{\phi_G^{bulk}} - 1. \tag{9}$$

Depletion is characterized by an adsorption thickness $\delta < 0$, while for adsorption $\delta > 0$. One could interpret δ as an effective amount of space gained ($\delta > 0$) or lost ($\delta < 0$) by the polymer due to presence of the hard surface. The neutral adsorption condition is characterized by a vanishing value of δ. The transition from negative (depletion) to positive adsorption occurs over a narrow $\Delta\chi$ range. We denote the particular affinity where δ vanishes as $\Delta\chi_n$. Note the highly non-linear behavior of δ near $\Delta\chi_n$ in the inset of Fig. 3. Previously, it has been argued that homopolymer accumulation at the solid interface occurs at $\Delta\chi \lesssim \ln(5/6) \approx -0.18$ [57]. In contrast, we define depletion as the situation at which $\delta < 0$ and adsorption in the case of $\delta > 0$.

One may question whether the transition from negative to positive adsorption depends on the polymer length N. In Fig. 4 we present the normalized adsorption thickness δ/R_g as a function of the effective colloid–polymer affinity $\Delta\chi$ for increasing polymer length N. As can be observed, the general dependence of the normalized adsorption thickness becomes stronger when the chain length N increases. Interestingly, however, the value of $\Delta\chi_n$, i.e. $\delta = 0$ (the dashed line), is rather insensitive to chain length. Thus, we focus on the case $N = 1000$ for the remainder of this work and will now pay attention to the polymer concentration effects. Furthermore, we note that at fixed $\Delta\chi$ the adsorption thickness depends on N. For adsorbed polymers ($\Delta\chi < -0.59$) this is in line with previous work which demonstrated that the adsorbed amount at saturation is dependent on the molar mass [52].

The polymer segment concentration profiles near a hard surface are modulated by the effective polymer–colloid affinity $\Delta\chi$, but also by the polymer bulk concentration ϕ_G^{bulk} and the polymer solvency χ_{GW}. Ultimately, polymer-mediated interactions are determined by the local polymer segment density profiles and by the osmotic pressure in the bulk. Independently of $\Delta\chi$, the osmotic pressure Π_{bulk} and consequently the fugacity of the polymers in bulk follows from FH theory [53]:

$$\tilde{\Pi}_{bulk} \equiv \frac{\Pi v_G}{k_BT} = -\frac{N}{\phi_G^*}\left[\ln\left(1-\phi_G^{bulk}\right) + \left(1-\frac{1}{N}\right)\phi_G^{bulk} + \chi_{GW}\left(\phi_G^{bulk}\right)^2\right], \tag{10}$$

[3] In the rest of this paper the term adsorption refers to positive adsorption, so to the case that the polymer chains are effectively adhesive or are attached at a surface; there is a positive excess of polymer chains at the surface with respect to the bulk concentration.

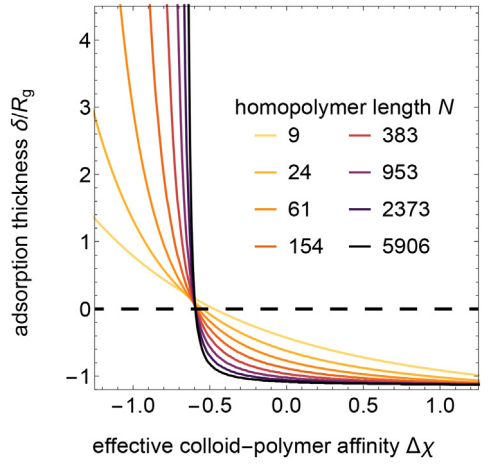

Fig. 4. Adsorption thickness as a function of the effective colloid–polymer affinity $\Delta\chi$ at very low polymer concentration $\phi_G^{bulk}/\phi_G^* = 10^{-7}$ with varying polymer length N as indicated. Dashed line marks neutral adsorption. Note that at sufficiently low polymer bulk concentrations δ does not depend on ϕ_G^{bulk}/ϕ_G^*.

which for polymers in a Θ-solvent ($\chi_{GW} = 0.5$) at low concentrations reduces to the Van 't Hoff law:

$$\tilde{\Pi}_{bulk} \approx \frac{\phi_G^{bulk}}{\phi_G^*}. \tag{11}$$

In Fig. 5, the dependence of δ on ϕ_G^{bulk} is presented for a wide range of effective polymer–surface affinities $\Delta\chi$. The information presented in Fig. 5 contains the dependence of Γ on $\Delta\chi$ and ϕ_{bulk}, as $\Gamma = \delta\phi_{bulk}/b^3$. For a polymer which is classically depleted [see Fig. 5(a)] from the surface we recover $\delta \approx -1.1R_g$ as expected [39] for $\phi_G^{bulk}/\phi_G^* \lesssim 0.05$. For all negative adsorption cases [$1 \lesssim \Delta\chi \lesssim -0.59$, see Fig. 5(a)], δ is nearly independent of ϕ_G^{bulk} for $\phi_G^{bulk}/\phi_G^* \lesssim 0.05$. For $\Delta\chi < 1$, the depletion thickness is always smaller than for the full depletion case due to a decreased free energy penalty of the guest polymer at the colloidal surface. For $\phi_G^{bulk}/\phi_G^* \gtrsim 0.05$, the bulk osmotic pressure exerted by the polymers on the depletion zone (the volume where polymers are depleted) leads to compression [30,55,58], and thus δ decreases in magnitude. This decrease of δ has been indirectly quantified experimentally for instance via optical tweezer [59] and atomic force microscopy measurements [22].

In the case of positive adsorption of homopolymers [$-0.59 \lesssim \Delta\chi \lesssim -0.82$, see Fig. 5(b)], the following trends are observed. A stronger effective segment–surface affinity (more negative $\Delta\chi$) results in a thicker adsorbed layer for all polymer bulk concentrations; i.e., a higher δ. As for the depletion attraction, δ eventually decreases in magnitude with increasing ϕ_G^{bulk}. Opposite to the depletion case, the regime where δ has a plateau value at low ϕ_G^{bulk} depends on the specific $\Delta\chi$-value: the lower $\Delta\chi$, the lower the ϕ_G^{bulk} at which the surface is saturated with adhering polymers.

The neutral adsorption condition is defined here in the dilute limit of ϕ_G^{bulk}. Remarkably, for $\Delta\chi = \Delta\chi_n$, δ becomes negative above $\phi_G^{bulk}/\phi_G^* \approx 0.01$, see Fig. 5. A negative δ-value indicates there is a depletion layer. The origin of this decrease of δ lies in the saturation of the surface with polymer. Therefore the concentration of polymer at the surface is no longer proportional to the bulk concentration and δ decreases. Although a depletion layer is formed, this process effectively resembles the decrease of δ observed in the positive adsorption case. Further increase of the polymer concentration leads to compression of the depletion layers due to solvent removal, which resembles the increase of δ for depleted polymers. This reflects the dual and intricate nature of the neutral adsorption condition, having both characteristics of depletion and adhesion.

Next, we focus on the concentration profiles in polymer solutions confined between two hard flat surfaces (Fig. 6). If the distance between the surfaces is large enough, the segment concentration profiles near either surface are like those reported in Fig. 3 near a single surface. For the depletion case, small interplate distances lead to a decrease of the maximum polymer concentration between plates with respect to the bulk due to an entropic penalty for polymers in confinement. In case of adsorbing polymers, the concentration between plates becomes larger than in bulk. The entropy loss of polymers in confinement is more than compensated by an enthalpic preference of the polymers to be in contact with the wall. Hence, when a free guest polymer chain can reach both surfaces ($h \approx 3R_g$, see Fig. 3) the polymer concentration is higher than in the bulk throughout the inter-plate region. Remarkably, in case of $\Delta\chi \approx -0.59$ the concentration profiles remain essentially flat and are equal to ϕ_G^{bulk} for all interplate distances. The small dents observed at the hard surfaces relate to the fact that a polymer can not be positioned inside the hard wall.

4. Pair interactions and second virial coefficient

In this section, the interactions between colloidal spheres mediated by the addition of homopolymers are studied at the two-body colloid–colloid interaction level. Examples of pair potentials between spherical colloids are shown in Fig. 7 at a low polymer bulk concentration ϕ_G^{bulk}. We focus first on classical depletion ($\Delta\chi = +1.0$), for which the attraction is strongest at $r = \sigma$ and vanishes at $r/\sigma \approx 1 + q$. The results are compared with the exact analytical expression for ideal nonadsorbing polymer chains by Eisenriegler [60]. The SCFT data points, the fitted solid HCY curve, and Eisenriegler's theoretical prediction (dashed grey curve) are in agreement. The interaction beyond the hard-core for $\Delta\chi$

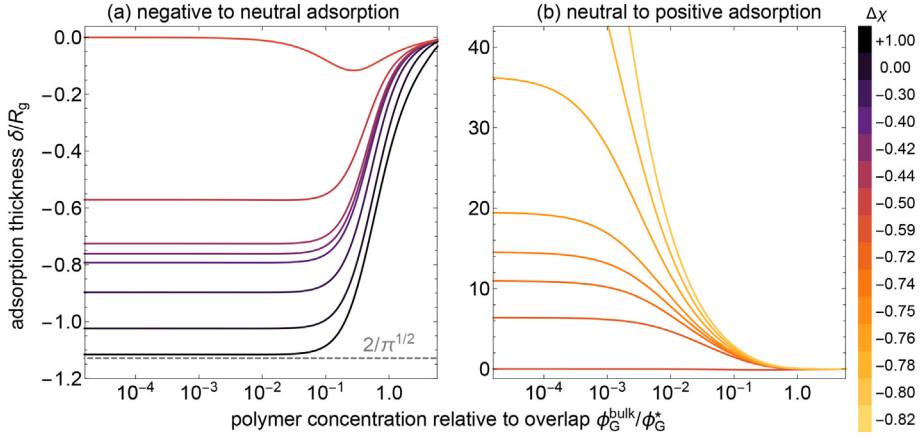

Fig. 5. Adsorption thickness δ as a function of the polymer bulk concentration relative to overlap (ϕ_G^{bulk}/ϕ_G^*) for a collection of effective polymer–colloid affinities ($\Delta\chi$) as indicated. At $\Delta\chi \approx -0.59$, the neutral adsorption condition holds, hence $\delta \approx 0$ up to relatively high polymer bulk concentrations.

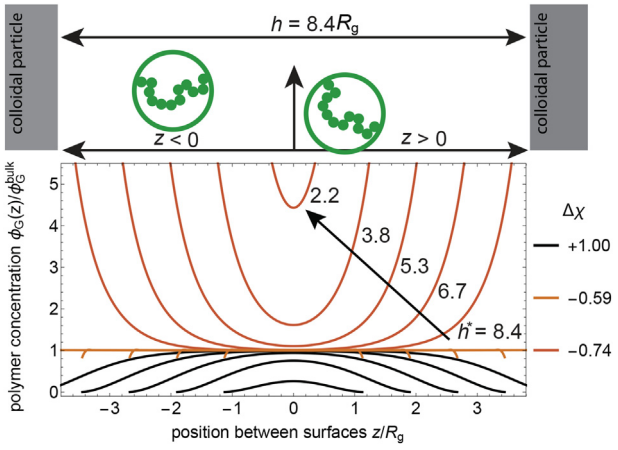

Fig. 6. Local polymer segment concentration profiles relative to bulk ϕ_G/ϕ_G^{bulk} as a function of the position z between two parallel, flat surfaces with decreasing the interplate-distance h (see sketch in the top panel). Effective polymer–colloid affinities $\Delta\chi$ are indicated on the right. Arrow indicates decreasing inter-plate distance, $h^* = h/R_g$.

≈ -0.59 is negligible: the colloidal particles interact effectively only via their excluded volume since there is neutral adsorption: inhomogeneities in the polymer segment density profiles are absent. When considering positive adsorption ($\Delta\chi = -0.74$) at low polymer bulk concentrations, the resulting attraction is shorter in range but significantly stronger than the depletion attraction. Due to the preference of the polymers to sit at the colloidal surface, bridging-induced attraction occurs due to weakly adsorbing polymers at low concentration. The different ranges of the depletion and bridging attractions presented are magnified in the inset in Fig. 7(b). For clarity, the fitted interactions are normalized by the absolute contact potential $|W(r=\sigma)|$. It follows that, for $\phi_G^{bulk}/\phi_G^* \lesssim 0.05$ the *normalized* depletion attraction remains fairly constant. Further details on the pair potentials with increasing ϕ_G^{bulk} and the results of the HCY fits are presented in Appendix B.

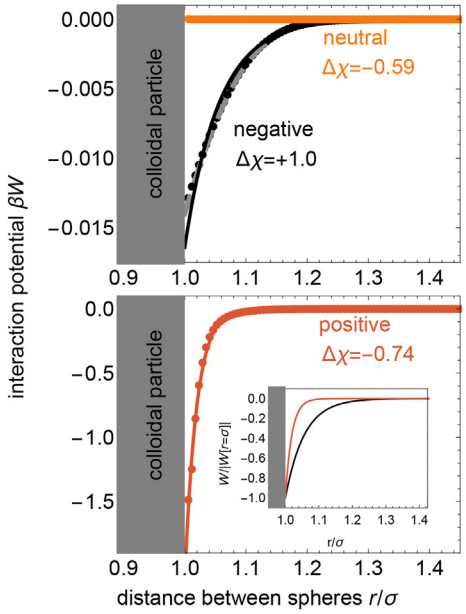

Fig. 7. Interaction between two spheres with diameter σ mediated by polymers with relative size $q \equiv 2R_g/\sigma = 0.15$ as a function of the distance between the centres of the spheres r. Effective polymer–colloid affinities $\Delta\chi$ are indicated. Solid curves correspond to the hard-core Yukawa (HCY) pair potential used to fit the calculated points. The dashed grey curve corresponds to theory by Eisenriegler [60] for the depletion attraction between two spheres. Polymer bulk concentration relative to overlap is $\phi_G^{bulk}/\phi_G^* = 10^{-3}$. Inset in the bottom panel shows the HCY-fitted depletion and adsorption potentials normalized by their absolute contact value $|W(r=\sigma)|$.

In a similar fashion as the adsorption thickness δ collects some key features of the concentration profiles, we use the second virial coefficient B_2 to analyze the overall effect of homopolymer addition on the pair–interactions. Often B_2 is used as an indicator of the phase stability of a colloidal suspension [61–64]. For pure HSs without additional interactions, $B_2^* \equiv B_2/v_c = 4$, with $v_c = (\pi/6)\sigma^3$ the colloidal particle volume. Conveniently, the HCY model fit provides information on how the range and the strength of the interaction depend on ϕ_G^{bulk}. The discussion which follows is based not only upon the pair interactions, but also on the information extracted from the HCY fit. The collected ranges q_Y and strengths ε of the attraction from this systematic fit are presented in Appendix B.

In Fig. 8(a), results for different polymer–colloid affinities, ranging from depletion ($\Delta\chi = +1.0$) or negative adsorption to neutral adsorption ($\Delta\chi \approx -0.59$), are plotted. Independently of the $\Delta\chi$-value, $B_2^* \approx 4$ for $\phi_G^{bulk}/\phi_G^* \lesssim 10^{-2}$. Further increase of ϕ_G^{bulk} first *decreases* B_2^* up to a minimum value around $\phi_G^{bulk}/\phi_G^* \approx 0.9$. The second virial coefficient then increases with ϕ_G^{bulk} back to $B_2^* \approx 4$. The depths of these minima in B_2^* decrease with decreasing $\Delta\chi$. The latter points towards a restabilisation of the colloidal suspension with decreasing $\Delta\chi$: the Vliegenthart–Lekkerkerker criterion [62] states that if B_2^* remains above -6, a colloidal dispersion is expected to be stable. Close to the neutral adsorption condition ($\Delta\chi \approx -0.59$), $B_2^* \approx 4$ for all ϕ_G^{bulk}, even though δ is small yet finite at intermediate polymer concentrations [$0.01 \lesssim \phi_G^{bulk}/\phi_G^* \lesssim 1$, see Fig. 5(a)].

In case of polymer adsorption onto the colloidal surface ($\Delta\chi \lesssim -0.59$), $B_2^* < 4$ already at very low polymer bulk concentrations. At a fixed, low ϕ_G^{bulk}, both the range and the strength of the bridging attraction *increase with decreasing* $\Delta\chi$ (see Appendix B). For lower $\Delta\chi$, the polymers stretch from one surface to the other in order to maximize their overall contact with the colloidal surfaces. As expected, the colloid–colloid attraction increases for higher effective affinity of the polymer chains to the colloidal surface. For $\phi_G^{bulk}/\phi_G^* \lesssim 0.1$, both the range and the strength of the adsorption increase with ϕ_G^{bulk}. As for the depletion cases, B_2^* also reaches a minimum with increasing ϕ_G^{bulk}. In this case, as polymer chains accumulate at the colloidal surface, competition between bridging attraction and steric (entropic) repulsion between adsorbed polymers takes place. A repulsive interaction beyond the hard-core occurs near and above ϕ_G^*, which results from a potential with a non-negligible attractive and very short-ranged strong repulsive contributions (see Fig. B.10, bottom-right panel). The trends obtained for B_2^* point, also for weakly adsorbing polymers, towards a destabilization–restabilization transition around $\phi_G^{bulk} \approx 0.1$. Similar trends with increasing bridging agent concentration for the second virial coefficient have been recently reported for sticky hard sphere binary mixtures [43,44]. Contrary to these approaches, we account specifically for the polymeric nature of the weakly adsorbing bridging agent.

5. Phase diagrams

Phase diagrams can be constructed from the SCFT approach combined with the Derjaguin approximation. The SCFT results for the pair interaction between two spheres were fitted to the hard core Yukawa (HCY) potential, which enables to compute the many-body Helmholtz energy by virtue of the first order mean spherical approximation (FMSA) [65,66]. Equal osmotic pressure $\tilde{\Pi}$ and chemical potential $\tilde{\mu}$ of the fluid and solid colloidal phases hold whenever phase coexistence takes place. Detailed results of the systematic fitting of the pair potentials can be found in Appendix B. As the FMSA considers interactions added to the hard sphere (HS) reference state, the well-known fluid–solid coexistence for HSs [67] is recovered for all $\Delta\chi$-values in absence of polymer ($\phi_G^{bulk} = 0$).

Predicted phase diagrams are shown in Fig. 9. For polymers which are fully depleted from the colloidal hard surface [$\phi_G(z=0) \approx 0$], the phase diagram matches predictions of the generalized free volume theory (GFVT) [28] for hard-spheres dispersed in a polymer solution

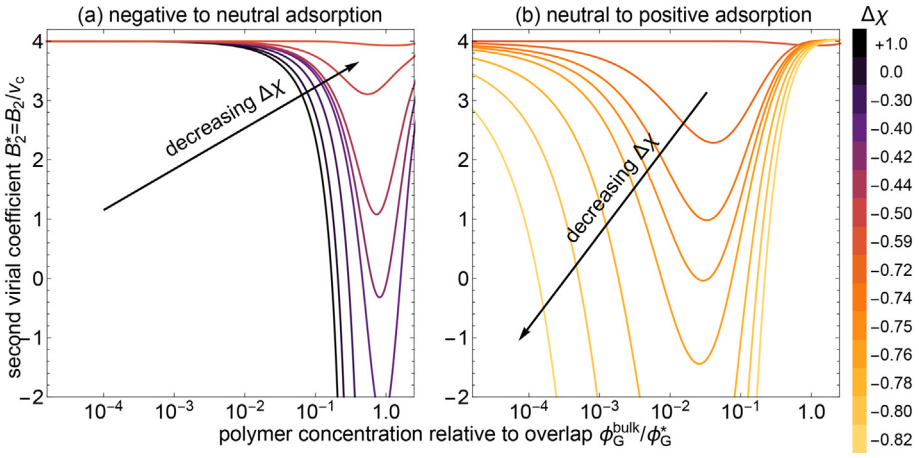

Fig. 8. Normalized second virial coefficient $B_2^* = B_2/v_c$ with increasing polymer bulk concentration ϕ_G^{bulk} relative to the polymer overlap concentration ϕ_G^*. The polymer–colloid affinities $\Delta\chi$ are indicated. For $\Delta\chi \approx -0.59$, the neutral adsorption case is retained, and thus $B_2^* \approx 4$ for a wide range of polymer concentrations.

at Θ-solvent conditions [see Fig. 9(a)]. Results from GFVT compare well with experimental results [28,29,36]. A significant decrease of $\Delta\chi$ is required in order to observe a shift of the fluid–solid binodal towards higher polymer concentration. Note how similar the phase diagrams are for $\Delta\chi = 1.0$ and $\Delta\chi = 0.0$. This corroborates the result that δ/R_g reaches a constant value with increasing $\Delta\chi$ (see inset of Fig. 3 for $\Delta\chi \gtrsim 0$). Further decreasing $\Delta\chi$ dramatically affects the fluid–solid binodal and increases the miscibility gap. For $\Delta\chi \approx -0.59$ the colloidal fluid–solid phase transition is only found at the coexisting concentrations expected for pure HS a polymer-free system. It is clear the concept of neutral adsorption reveals the possibility of realizing CPMs which are stable at high polymer and colloid concentrations.

At a fixed colloid concentration and $\Delta\chi$ (e.g., $\phi_c = 0.15$ and $\Delta\chi = -0.4$), depletion destabilization–restabilization with increasing ϕ_G^{bulk} is revealed: with increasing ϕ_G^{bulk}, the CPM goes from a stable one phase fluid to fluid–solid phase separation, and back to a single fluid phase [see Fig. 9(a)]. Similar trends have been observed in experiments where weaker depletion of polymer occurs due to the presence of short polymeric chains grafted to the colloidal particles [68,69]. It has been argued that a slight repulsive bump in the colloidal pair interaction for a strongly-depleted polymer may be sufficient to explain this restabilization [38,70,71]. Our SCF computations do reveal this repulsive bump in the depletion attraction [58] at sufficiently high ϕ_G^{bulk}, whose magnitude is however rather small compared to the contact potential (see Appendix B). These tiny repulsive barriers [30] do not play a major role in our model for restabilization.

Next, we pay attention to the phase diagrams obtained for weakly-adsorbing polymer [Fig. 9(b)]. Already at low ϕ_G^{bulk}, the (weakly) adsorbing polymers induce destabilization of the colloidal suspension. As expected from the ϕ_G^{bulk}-dependence of both δ and B_2, weak adsorption-driven F–S demixing of the CPM occurs at higher polymer

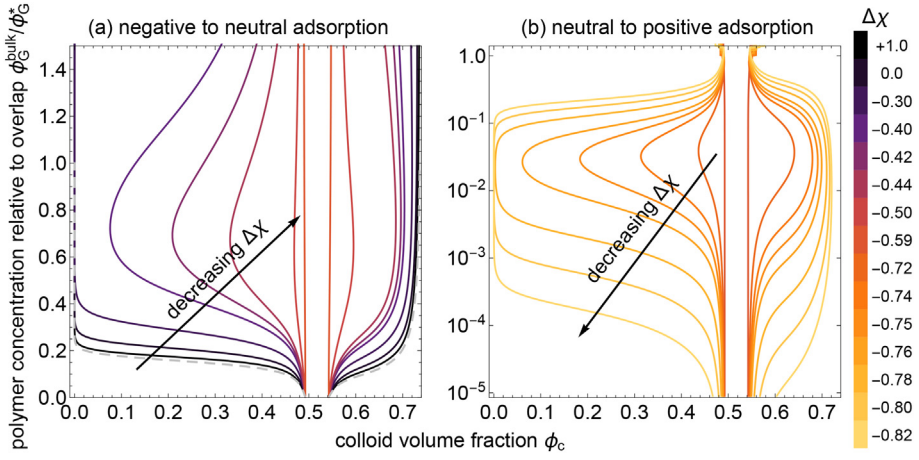

Fig. 9. Phase diagrams computed using hard-core Yukawa (HCY) fits to the SCF pair potentials, which were inserted into the free energy expressions from the first order mean spherical approximation to the HCY potential. Dashed grey curve corresponds to the phase diagram obtained using generalized free volume theory under Θ-solvent conditions. For $\Delta\chi \approx -0.59$ neutral adsorption takes place, and thus the colloidal fluid–solid coexistence remains at the same colloid volume fraction for all depletant concentrations.

Table 1
Depletion and weak adsorption characteristics as captured with our computations at low polymer concentration. The scaling exponent m varies from 0.142 to 0.083 and n from 0.212 to 0.140, for $\Delta\chi$ from −0.72 to −0.82.

	$\Delta\chi$	$\phi_G(z=0)/\phi_G^{bulk}$	δ/R_g	$\beta W(r=\sigma)$	range
Classic depletion	≈ 1	≈ 0	$= -2/\sqrt{\pi}$	$\sim \phi_G^{bulk}$	$\approx q$
Weak depletion	$\gtrsim -0.59$	< 1	$> -2/\sqrt{\pi}$	$\sim \phi_G^{bulk}$	$\lesssim q$
Neutral adsorption	≈ -0.59	≈ 1	≈ 0	≈ 0	≈ 0
Weak positive adsorption	$\lesssim -0.59$	> 1	> 0	$\sim (\phi_G^{bulk})^m$	$\sim (\phi_G^{bulk})^n$

concentration with increasing $\Delta\chi$. Further, the lower $\Delta\chi$, the smaller the stable one-phase region. Still, even at relatively small $\Delta\chi$ values (e.g., $\Delta\chi = -0.8$), restabilization occurs at high polymer concentration. Then the colloidal surfaces get saturated with (weakly) adsorbing polymers. Contrary to the depletion case, with decreasing $\Delta\chi$ the adsorption thickness does not reach a limiting value. To the best of our knowledge, there are no previously-reported phase diagrams for *weakly adsorbing* polymers in CPMs where the nature of the bridging agent is taken into account. It is noted, however, that our computations are based upon thermodynamic equilibrium. In case of bridging effects the interactions are quite strong, and kinetic, non-equilibrium phenomena also become important [25,45,72].

Yet another re-entrant phase behavior can be extracted from our framework, namely upon varying $\Delta\chi$. Provided that there is an experimentally realizable tuning parameter for the effective polymer–colloid affinity, a transition from negative to neutral to positive adsorption is expected, which consequently changes the phase stability. Temperature may for instance be such a tuning parameter. In fact, the transition here described from depletion to adsorption by changing the temperature has been reported recently [73]. We must note that in real life the solvency of the polymer also changes with temperature, which may make the phase diagram transitions even richer than with the simple model presented here. A perhaps simpler picture of the rich re-entrant phase behavior revealed in terms of the effective polymer–colloid affinity can be found in Appendix C.

6. Conclusions

The influence of polymer chains on colloidal stability has been reviewed and re-evaluated. First, an overview was presented of the consequences for colloidal stability in case of positive adsorption (accumulation of polymers at the colloidal surface) and negative adsorption (also termed depletion). We presented relatively simple computations which reveal the phase stability of colloid–polymer mixtures (CPMs) in the range from non-adsorbing (depleted) to weakly-adsorbed polymers. For classical depletion conditions, the results from the well-established generalized free volume theory are recovered for the depletant-to-colloid size ratio $q = 0.15$. Near a specific effective polymer–colloid affinity (the neutral adsorption condition), the CPM remains stable up to high polymer and colloid concentrations. This neutral adsorption condition does not significantly depend on polymer length. The developed framework captures the different nature of the depletion and bridging attractions between colloidal particles, summarized in Table 1.

Furthermore, it follows both from the second virial coefficient and from phase diagrams that a destabilization-restabilization-destabilization transition takes place as a function of the polymer bulk concentration when the colloid–polymer affinity is tuned from classical depletion to weak adsorption. The trends qualitatively match experimental observations on colloid–polymer mixtures.

Acknowledgement

This paper is dedicated to the memory of Hans Lyklema (1930–2017), who was an inspirational teacher and a charismatic scientist. Hans was a highly knowledgeable physical-chemist with a unique combination of broad and in-depth expertise, as highlighted in his book series on Fundamentals of Colloid and Interface Science (Elsevier, 1991-2005). He turned the Wageningen colloid group into a very strong laboratory with a few seminal lines of research. On all kinds of topics Hans was highly opinionated, including for instance on sustainability, the topic of a seminal lecture on the occasion of his official retirement in 1995. We are thankful for what he did for the scientists in our field. A.G.G. acknowledges funding from the NWO-TA project 731.015.205 by NWO, DSM, and SymoChem. M.V. acknowledges the Netherlands Organisation for Scientific Research (NWO) for a Veni grant (no. 722.017.005).

Declaration of Competing Interest

We confirm that there are no known conflicts of interest associated with this publication and there has been no significant financial support for this work that could have influenced its outcome. We confirm that the manuscript has been read and approved by all named authors and that there are no other persons who satisfied the criteria for authorship but are not listed. We further confirm that the order of authors listed in the manuscript has been approved by all of us.

We confirm that we have given due consideration to the protection of intellectual property associated with this work and that there are no impediments to publication, including the timing of publication, with respect to intellectual property. In so doing we confirm that we have followed the regulations of our institutions concerning intellectual property.

We understand that the Corresponding Author is the sole contact for the Editorial process (including Editorial Manager and direct communications with the office). He is responsible for communicating with the other authors about progress, submissions of revisions and final approval of proofs. We confirm that we have provided a current, correct email address which is accessible by the Corresponding Author and which has been configured to accept email from r.tuinier@tue.nl

Appendix A. FMSA for HCY potentials

The hard-core Yukawa HCY potential mimics a wide range of interactions between *spherical* particles, since both the range and strength can be tuned. It could represent, for instance, a screened double layer repulsion or a Van der Waals attraction between the colloids [74]. It is convenient to work with the dimensionless distance between the centres of two colloidal spheres $\tilde{r} \equiv r/\sigma$, with r the centre–to–centre distance and σ the colloidal diameter ($\sigma = 2R$, with R the colloidal sphere radius). A tilde over the quantities is used to indicate dimensionless units. The relative range of the Yukawa interaction is characterized by $q_Y = 2/(\hat{\kappa}\sigma)$, with $\hat{\kappa}$ the screening parameter (screening length $\hat{\kappa}^{-1}$). The HCY pair potential between colloidal spheres is written in terms of $\tilde{r}$, q_Y and ε, and normalized by $\beta = 1/(k_B T)$ (with k_B the Boltzmann constant and T the absolute temperature):

$$\beta W_{HCY} = \begin{cases} \infty & \text{for } \tilde{r}<1, \\ -\dfrac{\beta\varepsilon}{\tilde{r}} \exp\left[-\dfrac{2}{q_Y}(\tilde{r}-1)\right] & \text{for } \tilde{r}\geq 1. \end{cases} \tag{A.1}$$

The strength of the Yukawa potential is set via ε, defined such that $\varepsilon > 0$ implies a HCY attraction and $\varepsilon < 0$ a HCY repulsion. For $\varepsilon = 0$ the HCY reduces to the HS interaction:

$$\beta W_{HS} = \begin{cases} \infty & \text{for } \tilde{r}<1, \\ 0 & \text{for } \tilde{r}\geq 1. \end{cases} \tag{A.2}$$

Conveniently, from the HCY potential one can extract approximate (yet accurate) analytical thermodynamic expressions for the free energy of a HCY-interacting colloidal suspension (within certain limits) [65]. The free energy of a dispersion of colloidal spheres (F_c) interacting via hard-core Yukawa (F_{HCY}) is described as consisting of a hard core plus an additional Yukawa contribution [66,75]:

$$\frac{F_c v_c}{k_B T V} \equiv \tilde{F}_k^{HCY} = \tilde{F}_k^{HS} + \tilde{F}_Y, \tag{A.3}$$

where V is the volume of the system considered, and k denotes the phase-state (fluid or solid). The pure HS contributions to the free energy ($\tilde{F}_k^{HS}$) are well-known [76,77]. For a fluid of HSs, an accurate expression up to colloid volume fractions $\phi_c \approx 0.5$ follows from the Carnahan-Starling (CS) [77] equation of state (EOS):

$$\tilde{F}_{fluid}^{HS} = \phi_c\left(\ln\frac{\phi_c\Lambda_B^3}{v_c} - 1\right) + \frac{4\phi_c^2 - 3\phi_c^3}{(1-\phi_c)^2}, \tag{A.4}$$

where Λ_B is the de Broglie thermal wavelength. For a face-centred cubic (FCC) crystalline solid phase the Lennard-Jones–Devonshire (LJD) [76] EOS reads:

$$\tilde{F}_{solid}^{HS} = 2.1306\phi_c + 3\phi_c\ \ln\left(\frac{\phi_c}{1-\phi_c/\phi_c^{cp}}\right) + \phi_c\ \ln\left(\Lambda_B^3/v_c\right), \tag{A.5}$$

where $\phi_c^{cp} = \pi/(3\sqrt{2}) \approx 0.74$ is the volume fraction of HSs at close packing. The value 2.1306 has been collected from Monte Carlo simulations of the pure HS system [78], but is fairly close to the LJD solution.

Tang et al. [65] derived an expression for the free energy of a collection HCY spheres via a first-order mean spherical approximation (FMSA). The HCY potential allows an analytical solution of the Orstein–Zernike integral upon using the mean spherical closure approximation in Laplace space. This leads to analytical expressions for the radial distribution function and the direct correlation function up to first order in inverse temperature. The results provide a closed expression for F_Y in Eq. (A.3). Tang's approach can be extended to multi-Yukawa potentials, and has been successfully applied to study the interactions between charged colloidal particles [79] and to predict multi-body properties of particles interacting through a Lennard-Jones pair interaction [66]. This Yukawa contribution to the free energy can be written in a Van der Waals form [66,75]:

$$\tilde{F}_Y = -\gamma_Y\phi_c^2,$$

where the Van der Waals parameter γ_Y is not a constant but reads:

$$\gamma_Y = \gamma_1\beta\varepsilon + \gamma_2(\beta\varepsilon)^2, \tag{A.6}$$

in which the functions γ_1 and γ_2 can be expressed in terms of the auxiliary functions L_Y and Q_Y:

$$\gamma_1 = \frac{3q_Y^2 L_Y}{(1-\phi_c)^2(1+Q_Y)}, \quad \gamma_2 = \frac{3q_Y}{2(1+Q_Y)^4},$$

where

$$L_Y = 1 + 2/q_Y + \phi_c(2 + 1/q_Y),$$

and

$$Q_Y = \phi_c\frac{6(1-\phi_c)q_Y + 9\phi_c q_Y^2 - 3q_Y^3[1 + 2\phi_c - L_Y\ \exp(-2/q_Y)]}{2(1-\phi_c)^2}. \tag{A.7}$$

The osmotic pressure Π and chemical potential μ of HCY-interacting spheres follow from standard thermodynamic relations:

$$\beta\mu \equiv \tilde{\mu} = \left(\frac{\partial\tilde{F}_c}{\partial\phi_c}\right)_{T,V}, \quad \beta\Pi v_c \equiv \tilde{\Pi} = \phi_c\tilde{\mu} - \tilde{F}_c, \tag{A.8}$$

The relations in Eq. (A.8) apply in general, not only for interacting HCY spheres. Fluid–solid coexistence points at a fixed polymer bulk concentration are numerically evaluated by finding the colloid volume fractions at which the chemical potential and osmotic pressure of the fluid and solid phases are equal. Further improvements of Tang's FMSA have been proposed [80,81], yet lacking the simple and tractable closed forms presented here.

Appendix B. Pair potentials at various conditions

In Fig. B.10, we present pair potentials between colloidal (hard) spheres for various polymer bulk concentrations. The HCY model accurately describes the SCF computations for various polymer concentrations. In the right panel we zoom in the range of small interacting energies. For the depletion case, the small repulsive bump corresponds with the energy penalty of polymers escaping the depletion zone at high polymer concentrations. A tiny repulsive shoulder is also visible in case of neutral depletion at high polymer concentration. For the polymer adsorption cases, the strong and

very short-ranged repulsion observed at $r/\sigma \approx 1$ may point towards steric repulsion between adsorbed polymers; however we do not further discuss these effects as our main focus is on dilute polymer solutions.

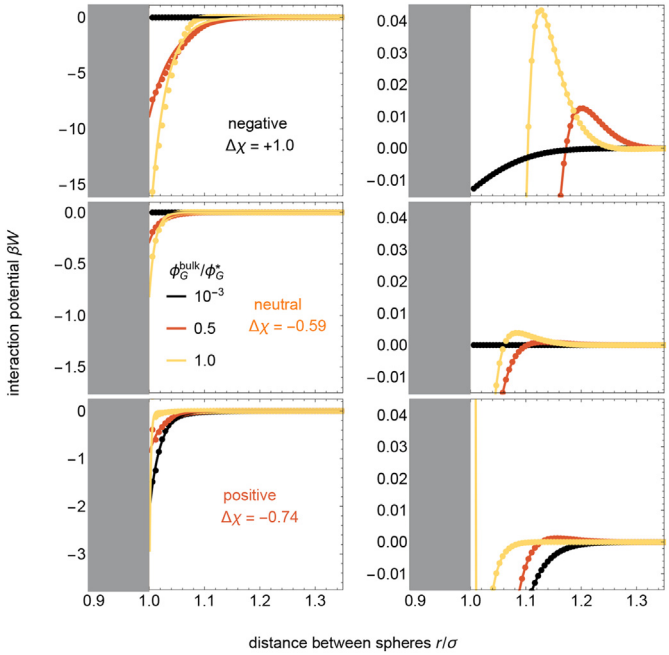

Fig. B.10. Interaction between spheres with diameter σ due to polymers with relative size $q \equiv 2R_g/\sigma = 0.15$ as a function of the distance between the centres of the spheres r/σ for the polymer–colloid affinities $\Delta\chi$ indicated. In the left panels, solid curves correspond to the hard-core Yukawa (HCY) pair potential used to fit the calculated points. In the right panels, solid curves are to guide the eye. Polymer bulk concentrations relative to overlap are indicated. Right panels zoom in on the range of small interaction energies for the potentials presented in the left panels.

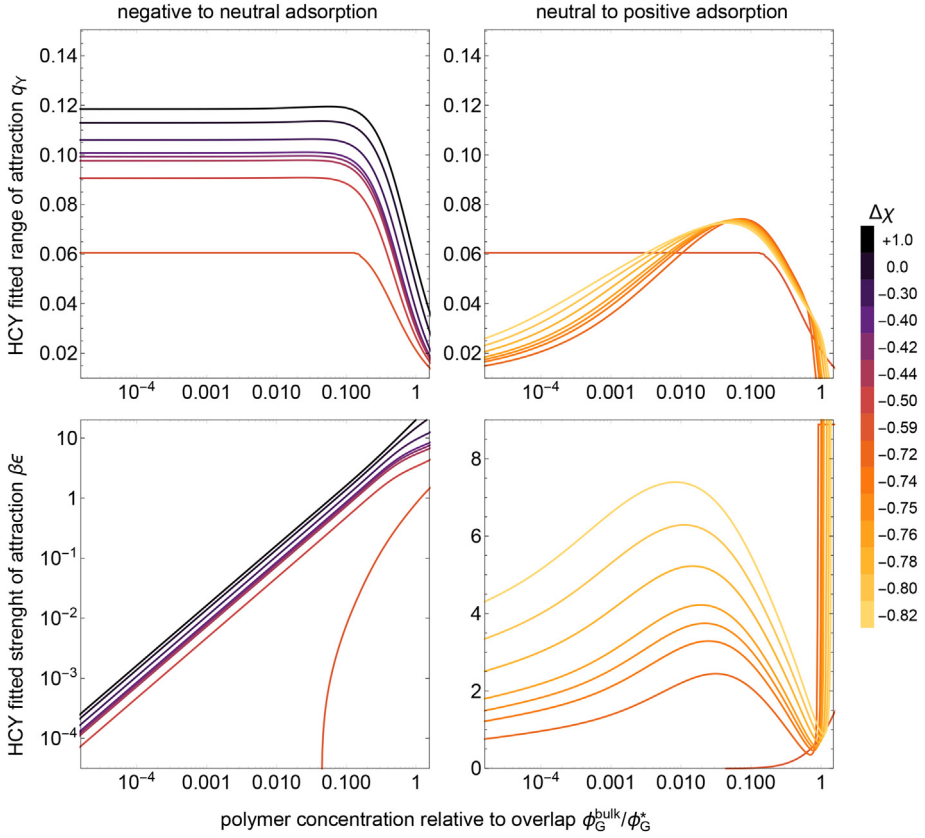

Fig. B.11. Fitted ranges q_Y and strengths ε of the HCY model with increasing polymer bulk concentration ϕ_G^{bulk} relative to overlap ϕ_G^* for different effective colloid–polymer affinities $\Delta\chi$ as indicated.

The results of the HCY-fitting leading to the phase diagrams are presented in Fig. B.11. The HCY-fits for the depletion cases show that q_Y is concentration-independent for the depletion attraction as expected in the dilute case ($\phi_G^{bulk}/\phi_G^* \lesssim 0.05$). Further, q_Y *decreases* above $\phi_G^{bulk}/\phi_G^* \approx$

0.05, corresponding to the compression of the depletion zones. On the other hand, the strength ε increases linearly with polymer concentration. Above $\phi_G^{bulk}/\phi_G^* \gtrsim 0.05$, the range decreases while its contact potential still increases.

In case of weak polymer adsorption, both the range q_Y and the strength ε of the bridging attraction increase with polymer bulk concentration for $\phi_G^{bulk}/\phi_G^* \lesssim 0.05$. Note that the maximum attraction strength shifts towards lower ϕ_G^{bulk} with decreasing $\Delta\chi$, again in accordance with what is observed for the adsorption thickness δ. The trends for adsorption around $\phi_G^{bulk}/\phi_G^* \approx 1$ point towards the limitations of fitting the SCF pair interactions with a single HCY potential. Phenomena such as the dramatic increase of ε accompanied by a decay of q_Y (observed in the right panels of Fig. B.10) point towards potentials as the yellow curve in the bottom right panel of Fig. B.10. From the trends on the range and strength of interactions at low ϕ_G^{bulk}, the relevance of the neutral adsorption condition becomes even clearer. While for depletion ε increases linearly and q_Y remains constant, for adsorption cases both ε and q_Y follow a power-law dependence with ϕ_G^{bulk}.

Appendix C. Re-entrant F–S phase behavior at fixed colloid volume fraction

In Fig. C.12 we present the phases present at fixed colloid volume fractions with increasing the polymer bulk concentration. Fig. C.12 provides further guiding on the explanation in the main text regarding the rich re-entrant phase behavior of the F–S phase separation.

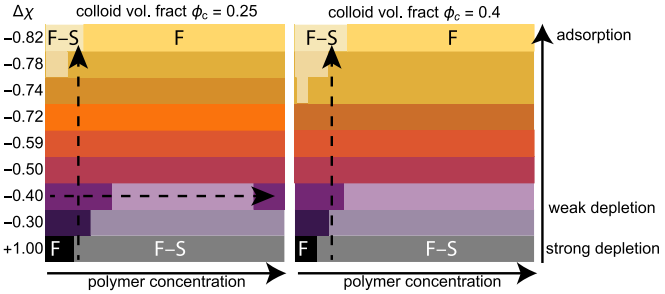

Fig. C.12. Re-entrant fluid–solid (F–S) phase behavior with increasing polymer concentration at fixed colloid volume fraction and varying the effective colloid–polymer affinity. Faded colors indicate F–S phase separation, solid colors stand for a single fluid phase as indicated for the case of classical depletion ($\Delta\chi = +1.00$) and adsorption ($\Delta\chi = -0.82$). Dashed arrows indicate the system parameter variations leading to re-entrant phase behavior of the fluid-solid phase separation.

References

[1] de Gennes PG, Badoz J. The Egyptian Scribe, Arabic Gum, and Chinese Ink. Springer-Verlag New York, Inc: Fragile Object; 1996.
[2] Derjaguin BV, Landau L. Acta Physicochim. USSR, 14; 1941.
[3] Verwey EJW, Overbeek JTG. Theory of the stability of lyophobic colloids. Amsterdam: Springer; 1948.
[4] Asakura S, Oosawa F. On interaction between two bodies immersed in a solution of macromolecules. J Chem Phys 1954;22:1255.
[5] Asakura S, Oosawa F. Interaction between particles suspended in solutions of macromolecules. J Polym Sci 1958;33:183–92.
[6] Fischer EW. Elektronenmikroskopische untersuchungen zur stabilitaet von suspensionen in makromolekularen loesungen. Kolloid-Zeitschrift 1958;160:120–41.
[7] Patat F, Killmann E, Schliebener C. Die adsorption von makromolekuelen aus loesung. Adv Polym Sci 1964;3:332–93.
[8] Fleer GJ. Polymer Adsorption and its Effect on Colloidal Stability: a Theoretical and Experimental Study on the Polyvinyl Alcohol-Silver Iodide System. PhD thesis. The Netherlands: Wageningen University; 1971.
[9] Fleer GJ, Koopal LK, Lyklema J. Polymer adsorption and its effect on the stability of hydrophobic colloids. Kolloid-Zeitschrift und Zeitschrift fuer Polymere 1972;250:689–702.
[10] Fleer GJ, Lyklema J. Polymer adsorption and its effect on the stability of hydrophobic colloids. ii. the flocculation process as studied with the silver iodide-polyvinyl alcohol system. J Colloid Interface Sci 1974;46:1–12.
[11] Fleer GJ, Lyklema J. Polymer adsorption and its effect on the stability of hydrophobic colloids. iii. kinetics of the flocculation of silver iodide sols. J Colloid Interface Sci 1976;55:228–38.
[12] Scheutjens JMHM, Fleer GJ. Statistical theory of the adsorption of interacting chain molecules. 1. partition function, segment density distribution, and adsorption isotherms. J Phys Chem 1979;83:1619–35.
[13] Scheutjens JMHM, Fleer GJ. Statistical theory of the adsorption of interacting chain molecules. 2. train, loop, and tail size distribution. J Phys Chem 1980;84:178–90.
[14] Fleer GJ. Polymers at interfaces and in colloidal dispersions. Adv Colloid Interf Sci 2010;159:99–116.
[15] Evers OA, Fleer GJ, Scheutjens JMHM, Lyklema J. Adsorption of weak polyelectrolytes from aqueous solution. J Colloid Interface Sci 1986;111:446–54.
[16] Lyklema J, Fleer GJ. Electrical contributions to the effect of macromolecules on colloid stability. Colloids Surf 1987;25:357–68.
[17] Mezzenga R, Schurtenberger P, Burbidge A, Michel M. Understanding foods as soft materials. Nat Mater 2005;4:729–40.
[18] Marenduzzo D, Finan K, Cook PR. The depletion attraction: an underappreciated force driving cellular organization. J Cell Biol 2006;175:681–6.
[19] Dickinson E. Exploring the frontiers of colloidal behavior where polymers and particles meet. Food Hydrocoll 2016;52:497–509.
[20] Tadros T. Colloids in paints. Ltd: John Wiley & Sons; 2011.
[21] Saha D, Bhattacharya S. Hydrocolloids as thickening and gelling agents in food: a critical review. J Food Sci Technol 2010;47:587–97.
[22] Wijting WK, Knoben W, Besseling NAM, Leermakers FAM, Cohen Stuart MA. Depletion interaction measured by colloidal probe atomic force microscopy. Phys Chem Chem Phys 2004;6:4432–9.
[23] Ouhajji S, Nylander T, Piculell L, Tuinier R, Linse P, Philipse AP. Depletion controlled surface deposition of uncharged colloidal spheres from stable bulk dispersions. Soft Matter 2016;12:3963–71.
[24] Xing X, Hua L, Ngai T. Depletion versus stabilization induced by polymers and nanoparticles: the state of the art. Curr Opin Colloid Interface Sci 2015;20:54–9.
[25] Gregory J, Barany S. Adsorption and flocculation by polymers and polymer mixtures. Adv Colloid Interf Sci 2011;169:1–12.
[26] Feigin RI, Napper DH. Stabilization of colloids by free polymer. J Colloid Interface Sci 1980;74:567–71.
[27] Feigin RI, Napper DH. Depletion stabilization and depletion flocculation. J Colloid Interface Sci 1980;75:525–41.
[28] Lekkerkerker HNW, Tuinier R. Colloids and the Depletion Interaction. Heidelberg: Springer; 2011.
[29] Fleer GJ, Tuinier R. Analytical phase diagrams for colloids and non-adsorbing polymer. Adv Colloid Interf Sci 2008;143:1–47.
[30] Bolhuis PG, Louis AA, Hansen JP, Meijer EJ. Accurate effective pair potentials for polymer solutions. J Chem Phys 2001;114:4296–311.
[31] Vrij A. Polymers at interfaces and the interactions in colloidal dispersions. Pure Appl Chem 1976;48:471–83.
[32] Li-in-on FKR, Vincent B, Waite FA. Stability of sterically stabilized dispersions at high polymer concentrations. ACS Symp Ser 1975;9:165–72.
[33] Pelssers EGM, Cohen Stuart MA, Fleer GJ. Kinetics of bridging flocculation. role of relaxations in the polymer layer. J Chem Soc Faraday Trans 1990;86:1355–61.
[34] Russel WB, Saville DA, Schowalter WR. Colloidal Dispersions. Cambridge Monographs on Mechanics: Cambridge University Press; 1989.
[35] McFarlane NL, Wagner NJ, Kaler EW, Lynch ML. Poly(ethylene oxide) (PEO) and poly (vinyl pyrolidone) (PVP) induce different changes in the colloid stability of nanoparticles. Langmuir 2010;26:13823–30.
[36] Aarts DGAL, Tuinier R, Lekkerkerker HNW. Phase behaviour of mixtures of colloidal spheres and excluded-volume polymer chains. J Phys Condens Matter 2002;14:7551–61.
[37] Surve M, Pryamitsyn V, Ganesan V. Depletion and pair interactions of proteins in polymer solutions. J Chem Phys 2005;122:154901.
[38] Semenov AN, Shvets AA. Theory of colloid depletion stabilization by unattached and adsorbed polymers. Soft Matter 2015;11:8863–78.

[39] Eisenriegler E. Dilute and semidilute polymer solutions near an adsorbing wall. J Chem Phys 1983;79:1052–64.
[40] Tuinier R, Ouhajji S, Linse P. Phase behaviour of colloids plus weakly adhesive polymers. Eur Phys J E 2016;39.
[41] Hooper JB, Schweizer KS. Theory of phase separation in polymer nanocomposites. Macromolecules 2006;39:5133–42.
[42] Surve M, Pryamitsyn V, Ganesan V. Nanoparticles in solutions of adsorbing polymers: pair interactions, percolation, and phase behavior. Langmuir 2006;22:969–81.
[43] Chen J, Kline SR, Liu Y. From the depletion attraction to the bridging attraction: the effect of solvent molecules on the effective colloidal interactions. J Chem Phys 2015; 142:084904.
[44] Fantoni R, Giacometti A, Santos A. Bridging and depletion mechanisms in colloid-colloid effective interactions: a reentrant phase diagram. J Chem Phys 2015;142: 224905.
[45] O'Shaughnessy B, Vavylonis D. Irreversible adsorption from dilute polymer solutions. Eur Phys J E 2003;11:213–30.
[46] Bergenholtz J, Poon WCK, Fuchs M. Gelation in model colloid-polymer mixtures. Langmuir 2003;19:4493–503.
[47] Zaccarelli E, Poon WCK. Colloidal glasses and gels: the interplay of bonding and caging. Proc Natl Acad Sci U S A 2009;106:15203–8.
[48] Scheutjens JMHM, Fleer GJ. Effect of polymer adsorption and depletion on the interaction between two parallel surfaces. Adv Colloid Interf Sci 1982;16:361–80.
[49] Scheutjens JMHM, Fleer GJ. Interaction between two adsorbed polymer layers. Macromolecules 1985;18:1882–900.
[50] Noro MG, Frenkel D. Extended corresponding-states behavior for particles with variable range attractions. J Chem Phys 2000;113:2941–4.
[51] Scheutjens JMHM, Fleer GJ. Statistical theory of the adsorption of interacting chain molecules. 2. train, loop, and tail size distribution. J Chem Phys 1980;84:178–90.
[52] Fleer GJ, Cohen Stuart MA, Scheutjens JMHM, Cosgrove T, Vincent B. Polymers at interfaces Springer Netherlands ; 1998.
[53] Flory PJ. Principles of polymer chemistry. Cornell University Press: The George Fisher Baker Non-Resident Lectureship in Chemistry at Cornell University; 1953.
[54] Mulero A, editor. Theory and simulations of hard-sphere fluids and related Sytems. Springer, Heidelberg: Lect. Notes Phys; 2008.
[55] Fleer GJ, Skvortsov AM, Tuinier R. Mean-field equation for the depletion thickness. Macromolecules 2003;36:7857–72.
[56] Harabagiu V, Sacarescu L, Farcas A, Pinteala M, Butnaru M. Surface-initiated polymerisation for nanocoatings. In: Makhlouf ASH, Tiginyanu I, editors. Nanocoatings and ultra-thin films. Woodhead Publishing: Woodhead Publishing Series in Metals and Surface Engineering; 2011. p. 78–130.
[57] Gorbunov AA, Skvortsov AM, van Male J, Fleer GJ. Mapping of continuum and lattice models for describing the adsorption of an ideal chain anchored to a planar surface. J Chem Phys 2001;114:5366–75.
[58] van der Gucht J, Besseling NAM. Interactions between surfaces in the presence of nonadsorbing equilibrium polymers. J Phys Condens Matter 2003;15:6627.
[59] Verma R, Crocker JC, Lubensky TC, Yodh AG. Attractions between hard colloidal spheres in semiflexible polymer solutions. Macromolecules 2000;33:177–86.
[60] Eisenriegler E. Universal density-force relations for polymers near a repulsive wall. Phys Rev E 1997;55:3116–23.
[61] Kurnaz ML, Maher JV. Measurement of the second virial coefficient for the interaction of dilute colloidal particles in a mixed solvent. Phys Rev E 1997;55:572.
[62] Vliegenthart GA, Lekkerkerker HNW. Predicting the gasliquid critical point from the second virial coefficient. J Chem Phys 2000;112:5364–9.
[63] Quigley A, Williams D. The second virial coefficient as a predictor of protein aggregation propensity: a self-interaction chromatography study. Eur J Pharm Biopharm 2015;96:282–90.
[64] Platten F, Hansen J-P, Wagner D, Egelhaaf SU. Second virial coefficient as determined from protein phase behavior. J Phys Chem Lett 2016;7:4008–14.
[65] Tang Y, Lu BC. A new solution of the Ornstein-Zernike equation from the perturbation theory. J Chem Phys 1993;99:9828–35.
[66] Tang Y, Lin Y-Z, Li Y-G. First-order mean spherical approximation for attractive, repulsive, and multi-Yukawa potentials. J Chem Phys 2005;122:184505.
[67] Hoover WG, Ree FH. Melting transition and communal entropy for hard spheres. J Chem Phys 1968;49:3609.
[68] Cowell C, Li-In-On R, Vincent B. Reversible flocculation of sterically-stabilised dispersions. J Chem Soc Faraday Trans 1978;1(74):337.
[69] Vincent B, Edwards J, Emmett S, Jones A. Depletion flocculation in dispersions of sterically-stabilised particles (soft spheres). Colloids Surf A Physicochem Eng Asp 1986;18:261–81.
[70] Semenov AN. Theory of colloid stabilization in semidilute polymer solutions. Macromolecules 2008;41:2243–9.
[71] Shvets AA, Semenov AN. Effective interactions between solid particles mediated by free polymer in solution. J Chem Phys 2013;139:054905.
[72] Van De Ven TGM. Kinetic aspects of polymer and polyelectrolyte adsorption on surfaces. Adv Colloid Interf Sci 1994;48:121–40.
[73] Feng L, Laderman B, Sacanna S, Chaikin P. Re-entrant solidification in polymercolloid mixtures as a consequence of competing entropic and enthalpic attractions. Nat Mater 2015;14:61–5.
[74] Fortini A, Dijkstra M, Tuinier R. Phase behaviour of charged colloidal sphere dispersions with added polymer chains. J Phys Condens Matter 2005;7783:25.
[75] Tuinier R, Fleer GJ. Critical endpoint and analytical phase diagram of attractive hard-core Yukawa spheres. J Phys Chem B 2006;110:20540–5.
[76] Lennard-Jones JE, Devonshire AF. Critical Phenomena in Gases. I. Proc R Soc A 1937; 163:53–70.
[77] Carnahan NF. Equation of state for nonattracting rigid spheres. J Chem Phys 1969; 51:635.
[78] Frenkel D, Ladd AJC. New Monte Carlo method to compute the free energy of arbitrary solids. Application to the fcc and hcp phases of hard spheres. J Chem Phys 1984;81:3188–93.
[79] Lin YZ, Li YG, Li JD. Study on multi-Yukawa potential between charged colloid particles. J Mol Liq 2006;125:29–36.
[80] Hlushak S, Trokhymchuk S, Nezbeda I. Improved first order mean spherical approximation for simple fluids. Condens Matter Phys 2011;14:33004.
[81] Hlushak S, Trokhymchuk A. Simplified exponential approximation for thermodynamics of a hard-core repulsive Yukawa fluid. Condens Matter Phys 2012;15:23003.